

**DESIGN AND SYNTHESIS OF BODIPY BASED  
PHOSGENE SENSOR**

**A Thesis Submitted to  
the Graduate School of Engineering and Sciences of  
İzmir Institute of Technology  
in Partial Fulfillment of the Requirements for the Degree of**

**MASTER OF SCIENCE**

**in Chemistry**

**by  
Melike SAYAR**

**June 2018  
İZMİR**

We approve the thesis of **MELİKE SAYAR**

**Examining Committee Members:**

---

**Assoc. Prof. Dr. Mustafa EMRULLAHOĞLU**  
Department of Chemistry, İzmir Institute of Technology

---

**Assoc. Prof. Dr. Murat IŞIK**  
Department of Food Engineering, Bingöl University

---

**Assoc. Prof. Dr. Yaşar AKDOĞAN**  
Department of Materials Science and Engineering, İzmir Institute of Technology

**21 June 2018**

---

**Assoc. Prof. Dr. Mustafa EMRULLAHOĞLU**  
Supervisor, Department of Chemistry  
İzmir Institute of Technology

---

**Prof. Dr. Ahmet Emin EROĞLU**  
Head of Department of Chemistry

---

**Prof. Dr. Aysun SOFUOĞLU**  
Dean of the Graduate School of  
Engineering and Sciences

## ACKNOWLEDGEMENTS

There are many people to thank who help, support and guidance during my study. Firstly, I would like to thank my supervisor, Assoc. Prof. Mustafa Emrullođlu for his patient, encouragement and understanding. It was a pleasure for me to join Emrullođlu research group and work on the most attractive field in chemistry which is fluorescent chemosensors and BODIPY chemistry under his guidance.

Also, I would like to thank all members of İYTE Emrullođlu research group especially Erman Karkuř, Muhammed Üçüncü, Ceyla Çetintař, Hüseyin Zeybek, Suay Dartar, Canan Üçüncü, Merve Çevik for their willingness to always help me.

Moreover, I would like to thank Dođan Taç and Fırat Zıyanak for their support and friendship.

I am also very grateful to my committee members, Assoc. Prof. Dr. Yařar Akdođan and Assoc. Prof. Dr. Murat Iřık. I really appreciate their precious time and continual support.

I want to thank my family for providing me all the moral support whenever I needed it the most. My parents, Tayyibe Sayar and İbrahim Sayar, and my sister Durseli Sayar.

Finally, I would like to thank Erman Kıbrıs for his everlasting encouragement and support.

# ABSTRACT

## DESIGN AND SYNTHESIS OF BODIPY BASED PHOSGENE SENSOR

Phosgene was used in World War I as a chemical warfare agent and now, it is used as only a chemical intermediate in the industrial field according to laws. Because of the result of exposure to phosgene, its detection plays a significant role to protect civilians against terrorist attacks, and also to warn people if there would be any leakage in industrial facilities.

To determine the phosgene, there are several methods like gas chromatography, which has several disadvantages such as poor portability and sensitivity and high cost or requiring of sophisticated procedures. However, fluorescence analysis has high sensitivity, resolution, and simplicity which provides real-time visual detection of analytes.

For this thesis, boron-dipyrromethene (BODIPY) dye was used as the signal reporter by synthesizing the new BODIPY derivative, to benefit from its outstanding photophysical properties. In addition to that, as the main purpose of this thesis, this is the first time an o-aminobenzyl amine group was used due to be the phosgene-specific reactive motif for research in phosgene sensing which is an investigation of photophysical properties of designed BODIPY derivative in the absence and presence of phosgene.

# ÖZET

## BODİPY BAZLI FOSGEN SENSÖRÜNÜN TASARIMI VE SENTEZİ

Fosgen, Birinci Dünya Savaşı'nda kimyasal savaş etmeni olarak kullanılmıştır ve şimdi yasalara göre sadece kimyasal ara ürün olarak endüstriyel alanlarda kullanılmaktadır. Fosgen salınımının sonuçları yüzünden, sivillerin terörist saldırılarına karşı korunması ve endüstriyel tesislerdeki herhangi bir kaçak olması durumunda insanları uyarmak için fosgenin tespiti önemli rol oynamaktadır.

Fosgeni tespit edebilmek için gaz kromatografisi gibi birçok yöntem bulunmaktadır. Bu yöntemler, zayıf taşınabilirlik ve hassaslık, yüksek maliyet veya komplike prosedürlere ihtiyaç duyma gibi birçok dezavantaja sahiptirler. Fakat, floresan analiz yöntemi, yüksek hassaslık, ayırma duyarlılığı ve basitliğe sahiptir. Bu özellikler, analitin eş zamanlı görsel tespitini sağlamaktadır.

Bu tez için, göze çarpan fotokimyasal özelliklerinden yararlanılarak yeni bir BODİPY türevi sentezlenmiş, boron-dipyrromethene (BODİPY) boyası sinyal habercisi olarak kullanılmıştır. Bunların yanısıra, tasarlanmış BODİPY türevinin, fosgen varlığı ve yokluğunda, fotofiziksel özelliklerinin fosgen duyarlılığının araştırılması için tezin ana amacı olarak, fosgene özel duyarlı birim olması nedeniyle ilk defa o-aminobenzil amin grubu kullanılmıştır.

# TABLE OF CONTENTS

LIST OF FIGURES .....	viii
ABBREVIATIONS .....	x
CHAPTER 1. INTRODUCTION .....	1
1.1. An Overview .....	1
1.2. Symmetric BODIPY Dyes .....	2
1.2.1. History and Structure .....	2
1.2.2. BODIPY as a Fluorophore .....	4
1.2.3. The Sensing Mechanism: Photoinduced Electron Transfer (PET) ...	5
1.3. Literature Work.....	6
CHAPTER 2. EXPERIMENTAL STUDY .....	12
2.1. General Methods .....	12
2.2. Details of Assay Experiments .....	12
2.3. Synthesis of Probe Molecule .....	12
2.3.1. Synthesis of Compound 1 .....	14
2.3.2. Synthesis of BOD-NH <sub>2</sub> .....	14
2.3.3. Synthesis of BOD-NO <sub>2</sub> .....	15
2.3.4. Synthesis of BOD-SYR .....	16
2.3.5. Synthesis of BOD-UREA .....	17
2.4. Determination of Quantum Yield .....	17
2.5. Determination of Detection Limit.....	18
CHAPTER 3. RESULT AND DISCUSSION .....	19
CHAPTER 4. CONCLUSION .....	24
REFERENCES .....	25

APPENDICES

APPENDIX A.  $^1\text{H}$ -NMR AND  $^{13}\text{C}$ -NMR SPECTRA OF COMPOUNDS..... 28

APPENDIX B. MASS SPECTRA OF COMPOUNDS ..... 34

## LIST OF FIGURES

<u>Figure</u>	<u>Page</u>
Figure 1.1. General Reaction of Phosgene .....	1
Figure 1.2. First synthesis of a boron dipyrroin dye by Treibs and Kreuzer .....	2
Figure 1.3. General synthesis of symmetric Fluoro Bodipy dyes. The base removes HF which is formed in the final step. ....	3
Figure 1.4. The two equivalent resonance structures are usually depicted as an uncharged form .....	3
Figure 1.5. The IUPAC Numbering System .....	4
Figure 1.6. Influence of alkyl and meso aryl Substituents on The Spectroscopic Properties (Source: Ni And Wu, 2014) .....	5
Figure 1.7. Photo Induced Electron Transfer Mechanism .....	6
Figure 1.8. General FRET Mechanism .....	6
Figure 1.9. FRET Based Probe for Detection of Phosgene .....	7
Figure 1.10. Rhodamine-Deoxylactam Based Sensor to Detect Phosgene .....	7
Figure 1.11. Sensing Mechanism of Sensor for the Detection of Phosgene .....	8
Figure 1.12. Emission band Difference between Phosgene and DCP .....	8
Figure 1.13. Structures of NBD-OPD, RB-OPD, and NAP-OPD .....	9
Figure 1.14. Chemical Structure of the Probe o-Pac and Proposed Sensing Mechanism	10
Figure 1.15. The Design Strategy of The Use of The Ratiometric Fluorescent Chemosensor, Phos-1, for Phosgene .....	10
Figure 1.16. Proposed Detection Mechanism with Phosgene .....	11
Figure 2.1. Stepwise synthesis of BOD-SYR. ....	13
Figure 2.2. 5,5-difluoro-1,3,7,9-tetramethyl-10-(4-nitrophenyl)-5H-4λ4,5λ4-dipyrrolo [1,2-c:2',1'-f][1,3,2]diazaborinine .....	14
Figure 2.3. 4-(5,5-difluoro-1,3,7,9-tetramethyl-5H-4λ4,5λ4-dipyrrolo[1,2-c:2',1'-f] [1,3,2]diazaborinin-10-yl)aniline .....	14
Figure 2.4. 4-(5,5-difluoro-1,3,7,9-tetramethyl-5H-4λ4,5λ4-dipyrrolo[1,2-c:2',1'- f][1,3,2] diazaborinin-10-yl)-N-(2-nitrobenzyl)aniline .....	15
Figure 2.5. N-(2-aminobenzyl)-4-(5,5-difluoro-1,3,7,9-tetramethyl-5H-4λ4,5λ4- dipyrrolo[1,2-c:2',1'-f][1,3,2]diazaborinin-10-yl)aniline .....	16



Figure 2.6.3-(4-(5,5-difluoro-1,3,7,9-tetramethyl-5H-4λ4,5λ4-dipyrrolo[1,2-c:2',1'-f] [1,3,2]diazaborinin-10-yl)phenyl)-3,4-dihydroquinazolin-2(1H)-one.....	17
Figure 3.1.Reaction-Based Detection of Phosgene .....	19
Figure 3.2.Absorbance and Fluorescence Spectra of BOD-SYR upon Gradual Addition of a Solution of Triphosgene (0–5 Equiv) in Acetonitrile (CH <sub>3</sub> CN), (λ <sub>ex</sub> =460 Nm). Inset: Fluorescence Response of <b>BOD-SYR</b> Towards Phosgene. ....	20
Figure 3.3.Naked eye Appearance in the Absence and the Presence of Phosgene.....	20
Figure 3.4.Time-Dependent Fluorescence Change <b>BOD-SYR</b> in CH <sub>3</sub> CN (20 Mm) in the Presence of Triphosgene (5 Equiv.) in CH <sub>3</sub> CN containing TEA (0.1%).....	21
Figure 3.5.Fluorescence Spectra of <b>BOD-SYR</b> in CH <sub>3</sub> CN (20 Mm) upon Gradual Addition of a Solution of Triphosgene (0–5 Equiv, From Bottom to Top) in CH <sub>3</sub> CN Containing TEA (0.1%). (λ <sub>ex</sub> = 460 Nm).....	21
Figure 3.6.Graphs Used for Calculation of Detection Limit .....	22
Figure 3.7.Proposed Reaction Mechanism for the Trapping of Triphosgene.....	23
Figure 3.8.Fluorescence intensity change of BOD-SYR (20 μM, in CH <sub>3</sub> CN/TEA (0.1%)) recorded 2 min. after the addition of various analytes (10 eq.) (λ <sub>ex</sub> = 460 nm). (1) Phosgene, (2) POCl <sub>3</sub> , (3) DCP, (4) (COCl) <sub>2</sub> , (5) SOCl <sub>2</sub> , (6) TsCl, (7) CH <sub>3</sub> COCl.....	23

## ABBREVIATIONS

<b>(COCl)<sub>2</sub></b>	Oxalyl chloride
<b>ABT</b>	Aminophenylbenzothiazole
<b>CAN</b>	Acetonitrile
<b>aq.</b>	Aqueous
<b>Ar</b>	Argon
<b>BF<sub>3</sub>.Et<sub>2</sub>O</b>	Boron trifluoride diethyl etherate
<b>BODIPY</b>	4,4-difluoro-4-bora-3a,4a-diaza-s-indacene
<b>CDCl<sub>3</sub></b>	Chloroform-d
<b>CH<sub>3</sub>CN</b>	Acetonitrile
<b>CH<sub>3</sub>COCl</b>	Acetyl chloride
<b>CHCl<sub>3</sub></b>	Chloroform
<b>DCM</b>	Dichloro methane
<b>DCP</b>	Diethylchlorophosphate
<b>DDQ</b>	2,3-Dichloro-5,6-dicyano-1,4-benzoquinone
<b>DMF</b>	Dimethylformamide
<b>equiv.</b>	Equivalent
<b>ESIPT</b>	Excited state intramolecular proton transfer
<b>Et<sub>3</sub>N</b>	Triethylamine
<b>EtOH</b>	Ethanol
<b>FRET</b>	Fluorescence Resonance Energy Transfer
<b>h</b>	Hour
<b>HCl</b>	Hydrochloric acid
<b>HF</b>	Hydrogen fluoride
<b>HOMO</b>	Highest Occupied Molecular Orbital
<b>ICT</b>	Intramolecular charge transfer
<b>K<sub>2</sub>CO<sub>3</sub></b>	Potassium carbonate
<b>LUMO</b>	Lowest Unoccupied Molecular Orbital
<b>M</b>	Molar
<b>MDI</b>	Methylenediphenyldiisocyanate

<b>mg</b>	Miligram
<b>MgSO<sub>4</sub></b>	Magnesium sulfate
<b>min.</b>	Minute
<b>mL</b>	Mililiter
<b>mmol</b>	Millimoles
<b>NH<sub>2</sub>NH<sub>2</sub>.H<sub>2</sub>O</b>	Hydrazine monohydrate
<b>NMR</b>	Nuclear magnetic resonance
<b>OPD</b>	o-Phenylenediamine
<b>Pd/C</b>	Palladium on carbon
<b>PET</b>	Photoinduced electron transfer
<b>POCl<sub>3</sub></b>	Phosphorous oxychloride
<b>ppb</b>	parts per billion
<b>ppm</b>	parts per million
<b>rt</b>	Room Temperature
<b>sec</b>	Second
<b>SOCl<sub>2</sub></b>	Thionyl chloride
<b>t</b>	Time
<b>TDI</b>	Toluene diisocyanate
<b>TEA</b>	Triethylamine
<b>TFA</b>	Trifluoroacetic acid
<b>THF</b>	Tetrahydrofuran
<b>TsCl</b>	Toluenesulfonyl chloride
<b>UV</b>	Ultraviolet

# CHAPTER 1

## INTRODUCTION

### 1.1. An Overview

Phosgene ( $\text{COCl}_2$ ) is a major industrial chemical used to make pesticides and chemicals such as methylenediphenyldiisocyanate (MDI) and toluene diisocyanate (TDI); however, at room temperature, it is a poisonous gas having an odor like that of musty hay which is produced by combining carbon monoxide and chlorine gases via a catalyst (activated carbon).

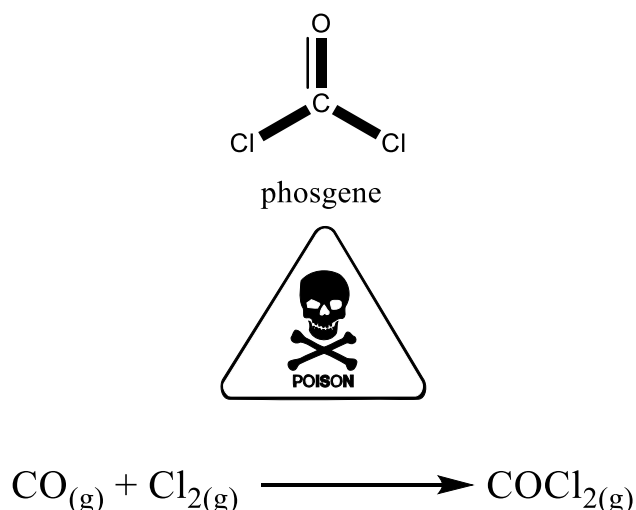


Figure 1.1. General Reaction of Phosgene

Phosgene was used extensively in World War I as an agent of chemical warfare. It is heavier than air and because of this, the vapour can stay near the ground and spread quickly. The result of exposure to phosgene may be noncardiogenic pulmonary edema or, pulmonary emphysema, both possibly leading to death (Bast and Glass 2009). Phosgene has an odor recognition threshold of 1.0 ppm, which is far higher than the safety margin of,  $\sim 0.6$  ppb and the full effects of phosgene inhalation appear several hours after exposure. Additionally, in contrast to other fatal nerve agents such as sarin, soman, and tabun that are rigorously controlled and prohibited by laws, phosgene is widely used as a

chemical intermediate in the industrial field. Therefore, its detection is significant not only to protect civilians against terrorist attacks but also to warn people against its leakage in industrial facilities (Cucinell and Arsenal 1974).

Conventional assays for phosgene, e.g. gas chromatography, are often limited by poor portability and high cost or by the requirement of sophisticated procedures. Fluorescence analysis has advantages in terms of sensitivity, resolution, and simplicity and also offers the possibility of real-time visual detection of analytes. Generally, detecting phosgene with a molecular probe involves trapping the molecule using a reactive site (e.g., hydroxy and amine functional groups), which is provided by a structural modification that generates a detectable optical signal (Chen et al. 2017).

## 1.2. Symmetric BODIPY Dyes

### 1.2.1. History and Structure

In 1968, Treibs and Kreuzer reported that although the acylated pyrrole **2** was desired from the acylation reaction of 2,4-dimethylpyrrole **1**, with acetic anhydride in the presence of boron trifluoride (used as a Lewis acid catalyst), highly fluorescent compound **4** was produced (Treibs and Kreuzer 1969). The compound derived from an acid catalyzed condensation of pyrroles **1** and **2** to dipyrin **3**, pursued by complexation with a boron difluoride unit to the dye **4** (Figure 1.2).

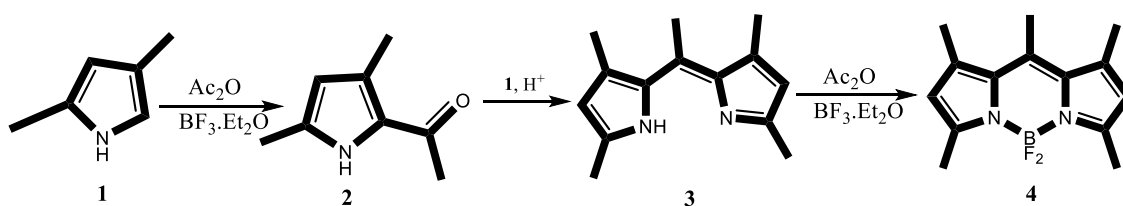


Figure 1.2 .The First synthesis of a boron dipyrin dye by Treibs and Kreuzer (Source: Treibs and Kreuzer 1969)

To establish the methane bridge between two pyrrole structures, a compound like acid anhydride, acyl chloride, or aldehyde which is highly electrophilic carbonyl compound can be used. To avoid polymerization and/or porphyrin formation, one of the non-

substituted pyrrole structures is usually substituted at one of the positions adjacent to the nitrogen atom whereas the other non-substituted pyrrole acts as a means of obtaining satisfactory yields of the corresponding naked dipyrromethene. After forming a complex with  $\text{BF}_3 \cdot \text{Et}_2\text{O}$  in the presence of a base, the isolation of symmetric F-Bodipy dyes by using any synthetic procedure that can be done rapidly as shown in Figure 1.3 (Ulrich, Ziessel, and Harriman 2008).

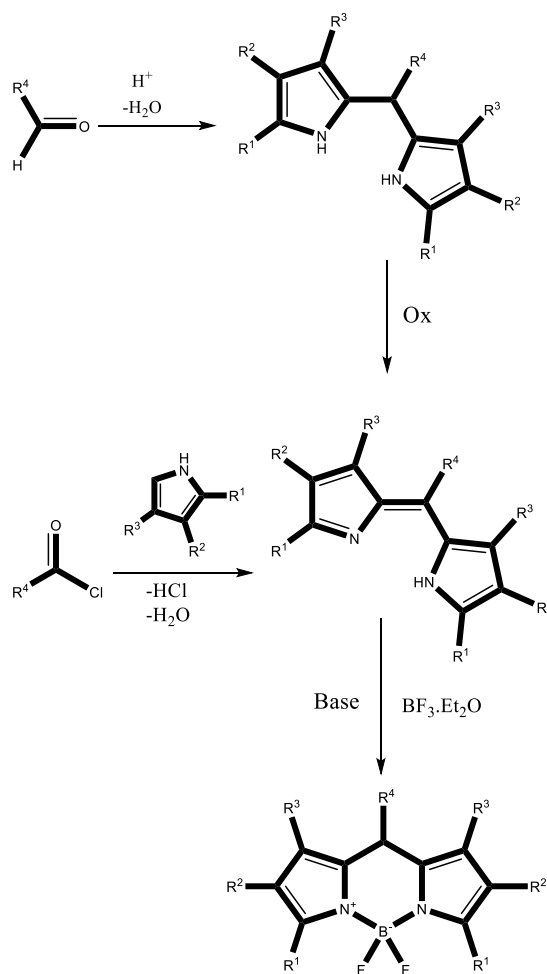


Figure 1.3. General synthesis of symmetric Fluoro Bodipy dyes. The base removes HF which is formed in the final step. (Source: Ulrich, Ziessel, and Harriman 2008)

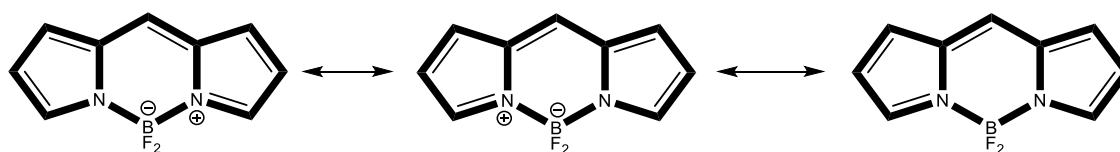


Figure 1.4. The two equivalent resonance structures are usually depicted as an uncharged form

The IUPAC numbering system for BODIPY dyes is different from the IUPAC numbering system for dipyrromethane and dipyririn. In all cases,  $\alpha, \beta$  and meso positions are designated in the same manner that the central carbon is called at meso position, the carbon which is adjacent to the nitrogen atom is called  $\alpha$ -position and the others are called  $\beta$  position (T. E. Wood and Thompson 2007).

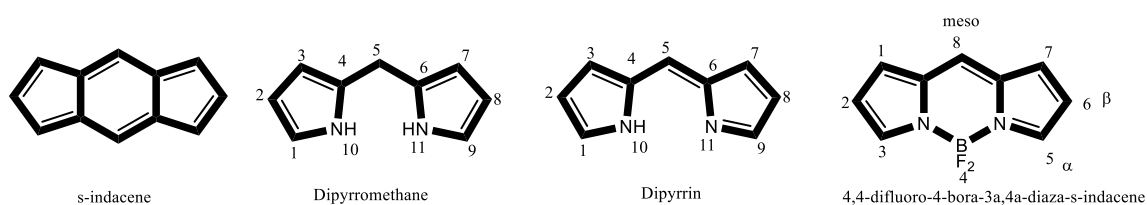


Figure 1.5. The IUPAC Numbering System (Source: Wood and Thompson 2007)

Various methodologies based on the well-known chemistry of pyrroles and dipyrromethanes like compound **3** (Figure 1.2) have been made advantage of in the synthesis of fluorophores. Incorporation of readily available pyrroles with highly electrophilic carbonyl compounds yields a variety of dipyrromethene ligands. Complexation with  $\text{BF}_3 \cdot \text{Et}_2\text{O}$  in the presence of a non-nucleophilic base (e.g secondary or tertiary amine), provides the BODIPY fluorophore in moderate, reproducible yields (Treibs and Kreuzer 1969).

### 1.2.2. BODIPY as a Fluorophore

Fluorescent probes have significance due to their developing applications and potential for allowing real-time studies that are the required by analytical chemistry, biochemistry, medicine, environmental science, etc.

Compounds, based on the 4,4-difluoro-4-bora-3a,4a-diaza-s-indacene core (hereafter referred to as BODIPY which is also its brand name) are generally dyes that absorb light in the visible range and are often fluorescent with high fluorescence quantum yields. Their absorption and emittance profiles tend to be relatively sharp and are only slightly Stokes shifted. The absorption- and fluorescence-spectroscopic properties of the Bodipy dyes are affected by the donor and acceptor characteristics of the pyrrole substituents (Loudet and Burgess 2007).

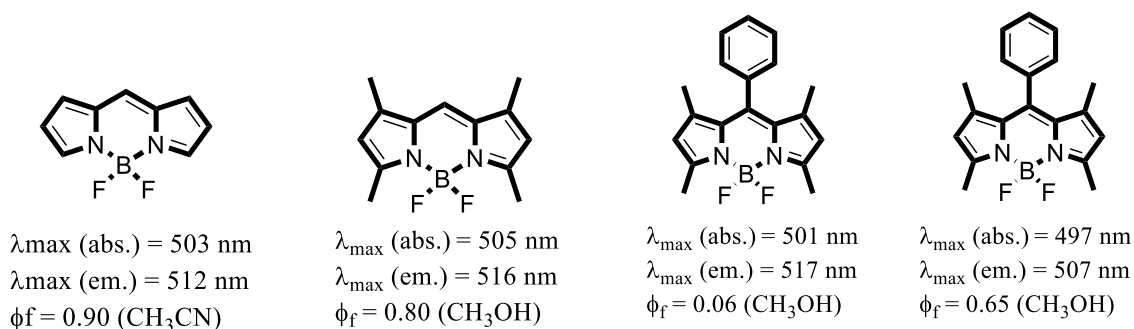


Figure 1.6. Influence of alkyl and meso aryl Substituents on The Spectroscopic Properties (Source: Ni and Wu, 2014)

BODIPY derivatives are uncharged, and their characteristics are mostly independent of solvent polarity. The complexes are stable against light and chemical reactions in the physiological pH-range, only decomposing in strong acidic and basic conditions (E. Wood 1994). These properties combine with a low toxicity to provide desirable advantages and consequently, BODIPY derivatives become excellent probes for use in biological systems and novel materials (Alford et al. 2009).

### 1.2.3. The Sensing Mechanism: Photoinduced Electron Transfer (PET)

The sensors which are based on a photoinduced electron transfer (PET) mechanism comprise the heteroatom with a nonbonding electron pair that quenches the fluorescence of a fluorophore unit in a polar environment by transferring the nonbonding electron pair to the excited fluorophore because of which the excited state energy is larger than the sum of the oxidation potential of the receptor and reduction potential of fluorophore. When the analyte bonds to the lone pairs of the receptor, the redox potential is increased. As a result of this, energy at the HOMO level is decreased and the PET process becomes invalid (Figure 1.7) (Das, Dutta, and Das 2013).



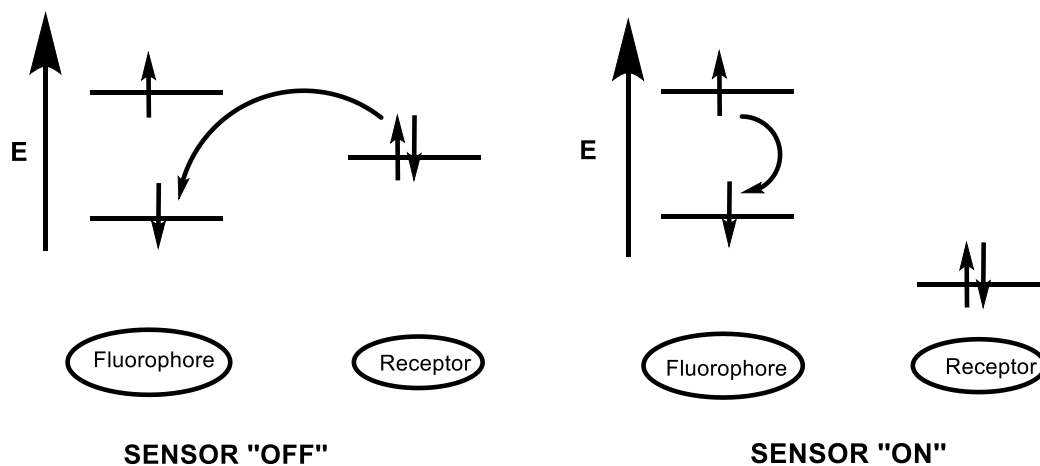


Figure 1.7. Photo-Induced Electron Transfer Mechanism  
(Source: Das, Dutta, and Das 2013)

### 1.3. Literature Work

Recent advances about the detection of phosgene have led to the contemporary approach to the design of molecular probes, especially for phosgene. Generally, the detection of phosgene with a fluorescent molecular probe comprises trapping the molecule by using its reactive site (e.g., a hydroxy and amine functional groups), generating modification as a detectable optical signal, (e.g., an observable colour change or change in fluorescence emission). The study of Rudkevich and co-workers is the first example of a fluorescent probe for detection of phosgene. They developed a coumarin derivatives by basing their functions on a fluorescence resonance energy transfer (FRET).

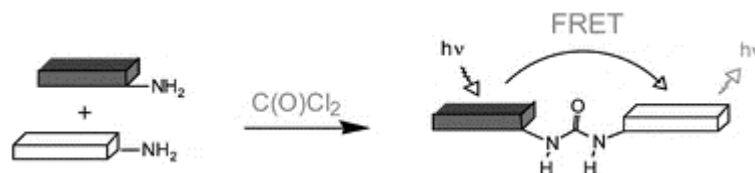


Figure 1.8. General FRET Mechanism (Source: Zhang and Rudkevich, 2007).

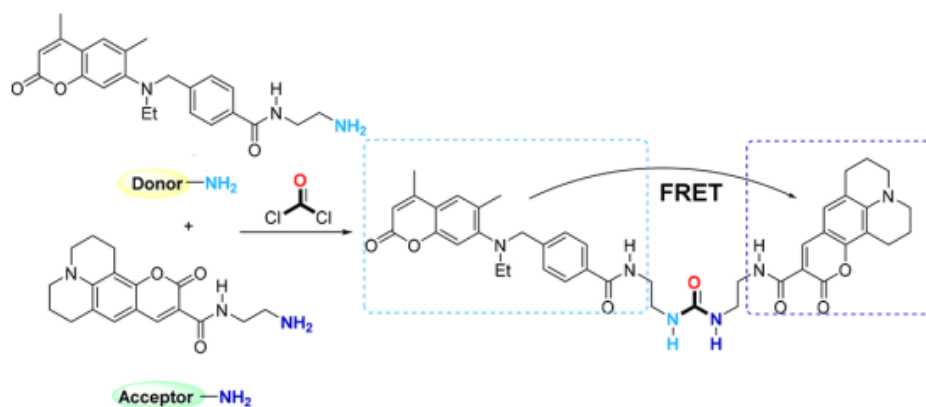


Figure 1.9. FRET-Based Probe for Detection of Phosgene  
(Source: Zhang and Rudkevich, 2007).

In this publication, one of the coumarin derivatives acted as a FRET donor fluorophore whereas the other one acted as a FRET acceptor fluorophore. When they reacted with phosgene, cross-linking was carried out. As a result of this reaction, a hybrid urea was formed, and this process caused a ratiometric change that when excited at 343 nm, led first to an emission increase at 464 nm, then to a decrease at 424 nm. However, it is hard to prevent donor-donor or acceptor-acceptor complex formation, that's why the sensitivity of the system is low (H. Zhang and Rudkevich 2007).

In 2012, Han and his co-workers developed a colourless and non-fluorescent phosgene chemosensor based on a rhodamine-deoxylactam structure. This chemosensor provides a fast color response that enables naked-eye detection, low background interference and high sensitivity (Wu et al. 2012).

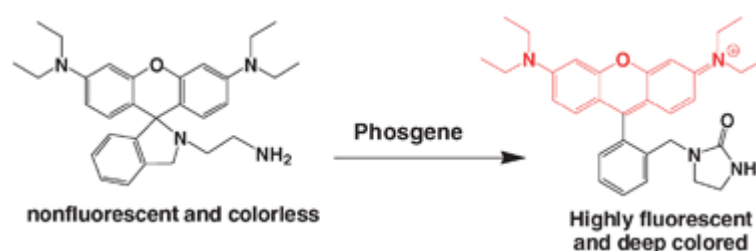


Figure 1.10. Rhodamine-Deoxylactam Based Sensor to Detect Phosgene  
(Source: Wu et al., 2012)

By using a similar concept of ethylenediamine recognition moiety, Tian et al. worked on 8-substituted BODIPY fluorophore. In the presence of phosgene, phosgene-mediated nucleophilic substitution and intramolecular cyclization are carried out in order

to form an imidazolone product. This is the first time, Tian et al. achieved as low a subnanomolar concentration level detection limit as 0,12nM.(Y. Zhang et al. 2017)

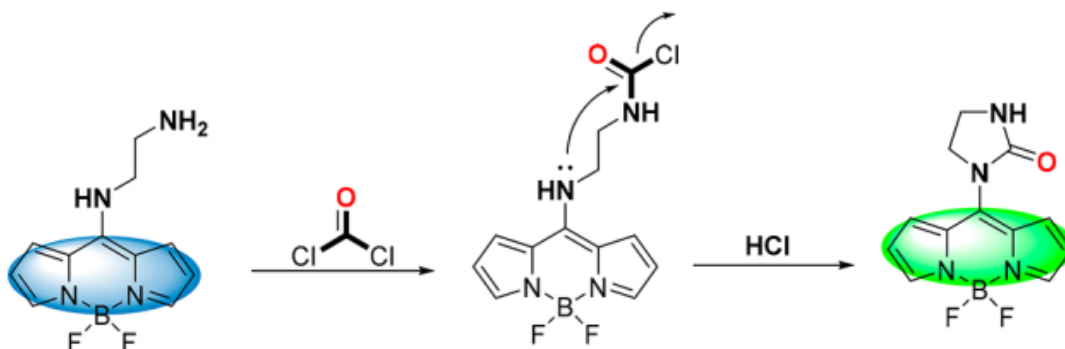


Figure 1.11.Sensing Mechanism of Sensor for the Detection of Phosgene  
(Source: Y. Zhang et al. 2017)

The above processes were carried out with hydroxyl or amine groups; however in order to differentiate phosgene and nerve gas agent, these methods are not really useful because if there are nerve agents that display the same nucleophilic substitution reaction behaviours, these methods are challengeable. The new fluorescent probe was developed by Yoon et al. to differentiate phosgene and nerve gas agents. This probe is based on pyronin, and it includes orto-phenylenediamine (OPD) that reacts with phosgene to produce benzimidazolone.

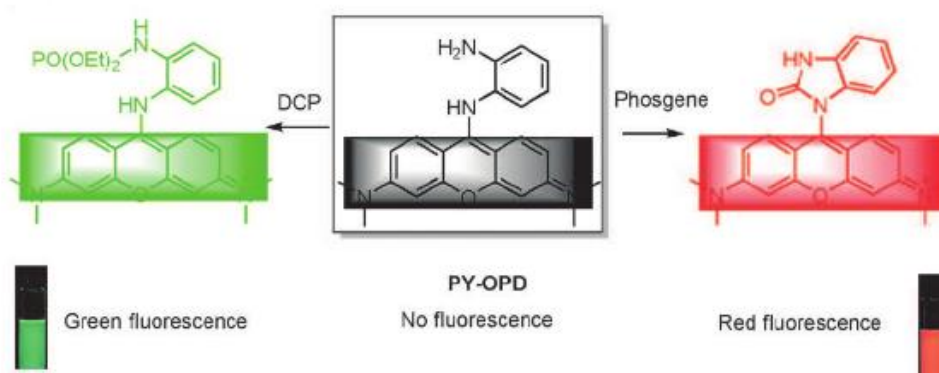


Figure 1.12.Emission band Difference between Phosgene and DCP  
(Source: Zhou et al., 2016)

During the reaction, the electron donating amine interacted with the electron withdrawing urea and as a result of this process, the PET mechanism was cancelled. When

PY-OPD is treated with phosgene, the color change can be observed with the naked eye and the emission band becomes red. However, if PY-OPD is treated with DCP, green fluorescence is observed because of the partial PET blocking. This work is the first in terms of differentiating the phosgene from nerve agents. (Zhou et al. 2016)

Moreover, by using OPD knowledge, Yoon et al. developed three OPD-based fluorescent probes for phosgene detection which include 4-chloro-7-nitrobenzo[c]-[1,2,5]oxadiazole (NBD), rhodamine (RB), and naphthalimide (NAP). When they are treated with phosgene, blue, green and red emissions are produced, respectively. Of particular interest, NBD-OPD turns the solution color from a dark orange to a pale yellow, and this change can be seen with the naked eye. By using an electrospinning technique, polymeric fibers can be seen with NBD-OPD and RB-OPD show significant fluorescence changes. (Hu et al. 2016)

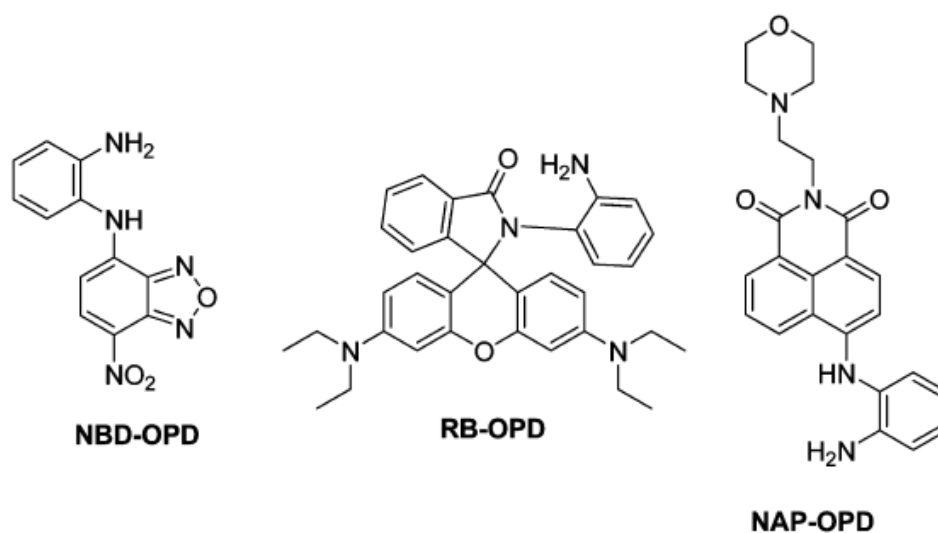


Figure 1.13. Structures of NBD-OPD, RB-OPD, and NAP-OPD (Source: Hu et al., 2016)

In a similar advance, Song et al. used coumarin dye with an OPD-reactive unit-based fluorophore. This sensor is very sensitive to nerve agent mimics and other acyl chlorides. Also its detection is very fast, in a one min detection process finishes with a detection limit as 3 nM. (Xia, Xu, and Song 2017)

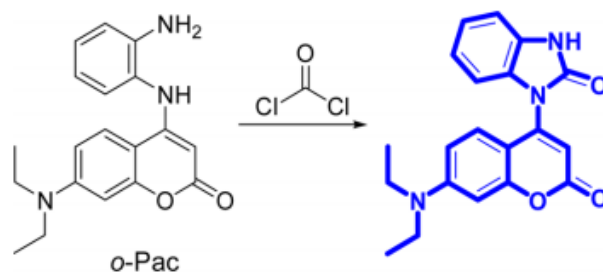


Figure 1.14. Chemical Structure of the Probe o-Pac and Proposed Sensing Mechanism (Source: Xia, Xu, and Song, 2017)

Additionally, Song et al. developed a fluorescent chemosensor containing 4,5-diamino-1,8-Naphthalimide. By treating this compound with phosgene, the intramolecular charge-transfer (ICT) property was found to get a ratiometric fluorescent response. The color change which is from green to blue, can be easily seen with the naked eye. This is the first work that used a ratiometric fluorescent sensor with low detection limit to produce a visual color change. (Wang, Zhong, and Song 2017)

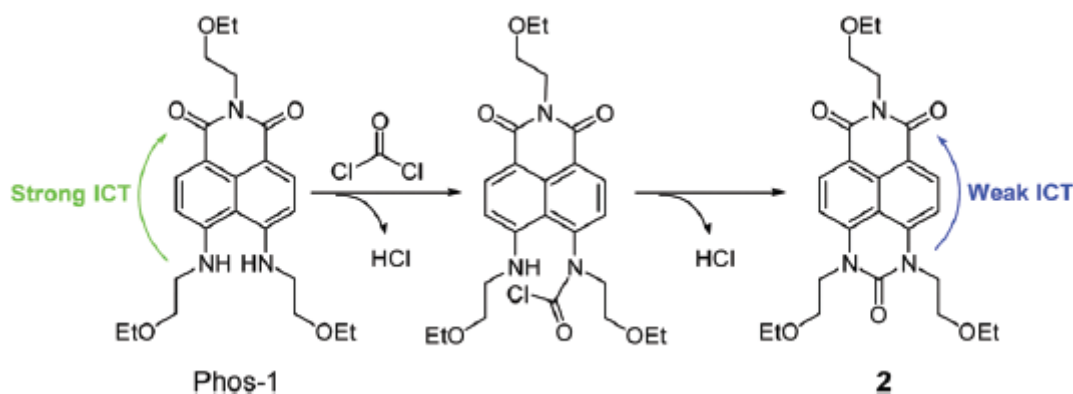


Figure 1.15. The Design Strategy of The Use of The Ratiometric Fluorescent Chemosensor, Phos-1, for Phosgene (Source: Wang, Zhong, and Song 2017)

In order to mitigate interference from other species like nitric oxide, Yoon et al. improved sensor molecule 2-(2-(ABT)), which is based on excited state intramolecular proton transfer (ESIPT).

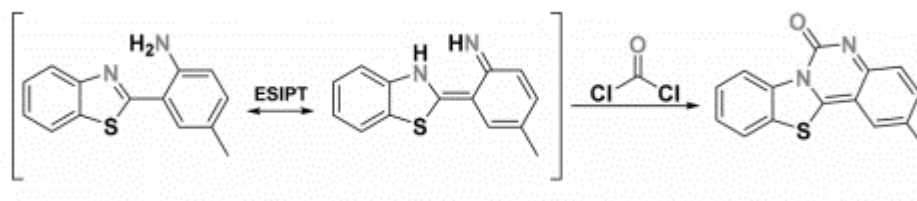


Figure 1.16. Proposed Detection Mechanism with Phosgene (Source: Chen et al. 2017)

Under an ES IPT process, dual sites are produced to react with phosgene, and as a result of treating with phosgene, there are both colorimetric and ratiometric change. Colorimetric change is from colorless to yellow, whereas fluorescent color change is from blue to green. (Chen et al. 2017)

## CHAPTER 2

### EXPERIMENTAL STUDY

#### 2.1. General Methods

All reagents were purchased from commercial suppliers (Aldrich and Merck) and used without further purification.  $^1\text{H}$  NMR and  $^{13}\text{C}$  NMR were measured on a Varian VNMRJ 400 Nuclear Magnetic Resonance Spectrometer. UV absorption spectra was obtained on Shimadzu UV-2550 Spectrophotometer. Fluorescence emission spectra was obtained using Varian Cary Eclipse Fluorescence Spectrophotometer. Samples were contained in 10.0 mm path length quartz cuvettes (2.0 mL volume). Upon excitation at 460 nm, the emission spectra were integrated over the range 480 nm to 700 nm (Both excitation and emission slit width 5 nm / 5 nm).

#### 2.2. Details of Assay Experiments

In order to avoid handling volatile phosgene during the titration experiments, we employed nonvolatile and less toxic counterpart triphosgene ( $\text{CCl}_3\text{OC}(\text{O})\text{OCCl}_3$ ), which is a well-known precursor that generates phosgene in the presence of tertiary amines in solutions. For all measurements in solutions, acetonitrile ( $\text{CH}_3\text{CN}$ ) was employed as the solvent.

#### 2.3. Synthesis of Probe Molecule

The stepwise synthesis for BOD-NH<sub>2</sub> and BOD-SYR was shown in Figure 2.1. Compound 1 was synthesized by using literature procedure.

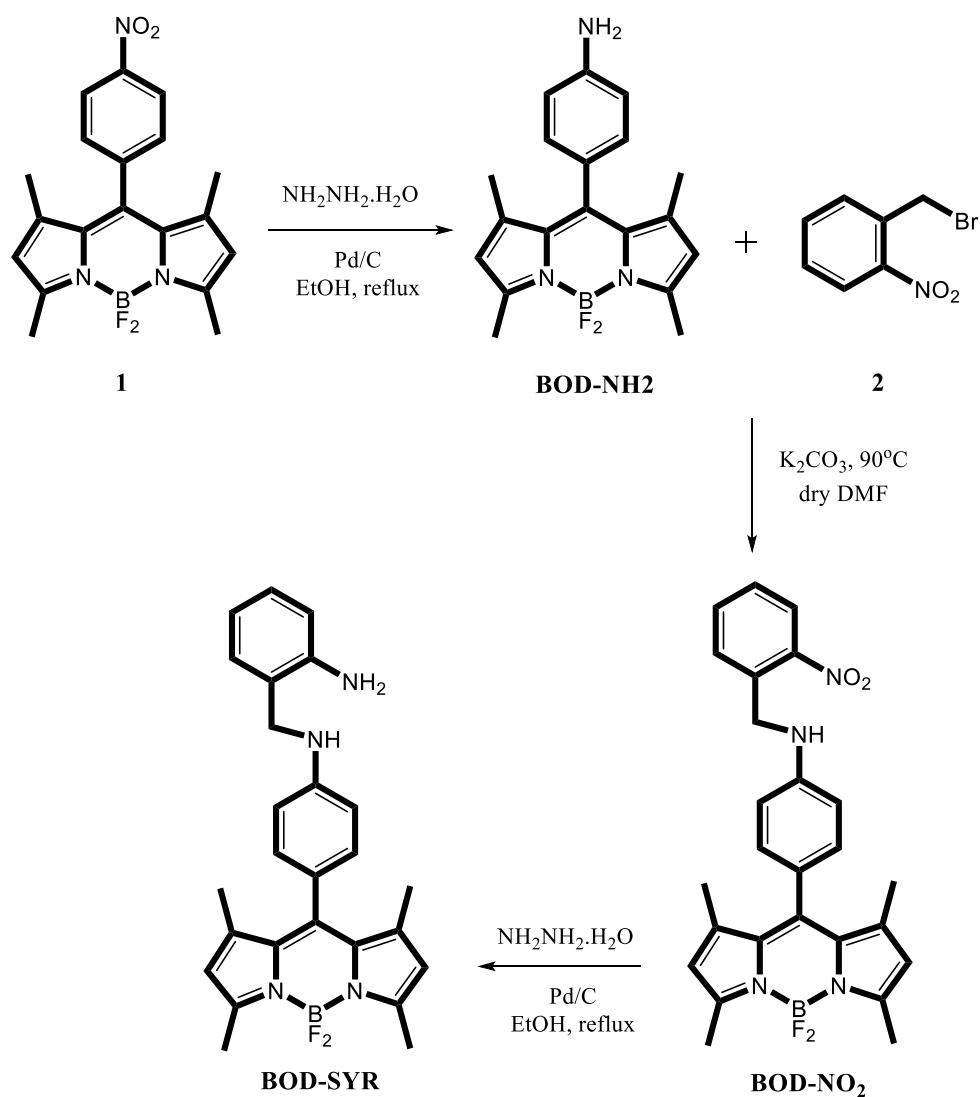


Figure 2.1. Stepwise synthesis of BOD-SYR.

The stepwise synthesis of the BOD-SYR is shown in Fig 2.1. As can be seen, a BODIPY dye derivative is obtained with a free amine, **BOD-NH<sub>2</sub>**, by reducing its meso-NO<sub>2</sub>-phenyl moiety. Further alkylation of **BOD-NH<sub>2</sub>** is carried out with the individually produced molecule, as written in the literature, Compound **2**. As a last step of the pathway, reduction process undergoes to form the probe compound, **BOD-SYR**.



### 2.3.1. Synthesis of Compound 1

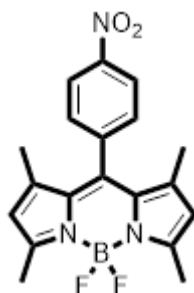


Figure 2.2. 5,5-difluoro-1,3,7,9-tetramethyl-10-(4-nitrophenyl)-5H-4 $\lambda$ 4,5 $\lambda$ 4-dipyrrolo [1,2-c:2',1'-f][1,3,2]diazaborinine

**5,5-difluoro-1,3,7,9-tetramethyl-10-(4-nitrophenyl)-5H-4 $\lambda$ 4,5 $\lambda$ 4-dipyrrolo [1,2-c:2',1'-f][1,3,2]diazaborinine:** 2,4-dimethylpyrrole (413 mL, 4mmol) was dissolved in 25mL dry THF and after that, p-nitrobenzaldehyde (300mg, 2mmol) was added. Then, 60 mL TFA was added and the colour became light brown. After 16 hours, DDQ (455 mg, 2mmol) was dissolved in 15 mL dry THF and added to reaction medium drop by drop in ice. After 4 hours stirring, TEA (12mL) was added dropwise in ice. After 45 min. stirring, 12mL BF<sub>3</sub>.Et<sub>2</sub>O was added by using dropping funnel. It was left overnight, and the resulting solution was extracted with DCM (3x30mL) and dried over MgSO<sub>4</sub>. It was used for the next step without further any purification.

### 2.3.2. Synthesis of BOD-NH<sub>2</sub>

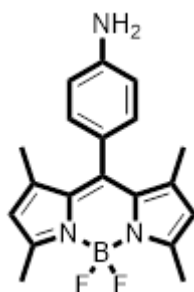


Figure 2.3. 4-(5,5-difluoro-1,3,7,9-tetramethyl-5H-4 $\lambda$ 4,5 $\lambda$ 4-dipyrrolo[1,2-c:2',1'-f][1,3,2]diazaborinin-10-yl)aniline

To a solution of 5,5-difluoro-1,3,7,9-tetramethyl-10-(4-nitrophenyl)-5*H*-4 $\lambda$ 4,5 $\lambda$ 4-dipyrrolo[1,2-*c*:2',1'-*f*][1,3,2]diazaborinine (100mg, 0.29 mmol) in EtOH (20mL) were added NH<sub>2</sub>NH<sub>2</sub>.H<sub>2</sub>O (250 $\mu$ L) and Pd/C (26.6mg, 0.025 mmol). The reaction mixture was heated at reflux temperature under Ar atmosphere for two hours, then it was cooled to room temperature and filtered. The solids were washed with DCM. The resultant residue was purified by column chromatography (2:1 (Hexane:Ethyl acetate) to afford **BOD-NH<sub>2</sub>** as dark red solid (50 mg, 50 % yield). <sup>1</sup>H NMR (400 MHz, CDCl<sub>3</sub>)  $\delta$  = 7.02 (td, *J* = 2.3, 8.6 Hz, 2 H), 6.79 (td, *J* = 2.3, 8.2 Hz, 2 H), 5.98 (s, 2 H), 3.84 (br. s., 2 H), 2.55 (s, 6 H), 1.50 (s, 6 H). <sup>13</sup>C NMR (100 MHz, CDCl<sub>3</sub>)  $\delta$  = 154.9, 147.0, 143.2, 142.6, 132.0, 130.4, 128.9, 124.7, 120.9, 115.4, 110.0, 14.7, 14.6.

### 2.3.3. Synthesis of BOD-NO<sub>2</sub>

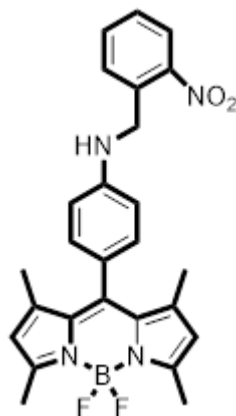


Figure 2.4.4-(5,5-difluoro-1,3,7,9-tetramethyl-5*H*-4 $\lambda$ 4,5 $\lambda$ 4-dipyrrolo[1,2-*c*:2',1'-*f*][1,3,2]diazaborinin-10-yl)-*N*-(2-nitrobenzyl)aniline

**4-(5,5-difluoro-1,3,7,9-tetramethyl-5*H*-4 $\lambda$ 4,5 $\lambda$ 4-dipyrrolo[1,2-*c*:2',1'-*f*][1,3,2]diazaborinin-10-yl)-*N*-(2-nitrobenzyl)aniline:** BOD-NH<sub>2</sub> (33mg, 0.1mmol) was dissolved in dry DMF (4mL). Then, 1-(bromomethyl)-2-nitrobenzene (50.6mg, 0.23mmol) was added to solution. After that, K<sub>2</sub>CO<sub>3</sub> (17mg, 0.12mmol) was added into the solution. The reaction mixture was heated at 90°C under Ar. It was used for the next step without further any purification.

### 2.3.4. Synthesis of BOD-SYR

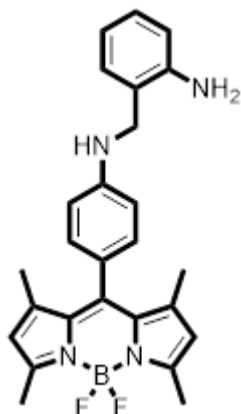


Figure 2.5. *N*-(2-aminobenzyl)-4-(5,5-difluoro-1,3,7,9-tetramethyl-5H-4λ<sup>4</sup>, 5λ<sup>4</sup>-dipyrrolo [1,2-c:2',1'-f][1,3,2]diazaborinin-10-yl)aniline

***N*-(2-aminobenzyl)-4-(5,5-difluoro-1,3,7,9-tetramethyl-5H-4λ<sup>4</sup>,5λ<sup>4</sup>-dipyrrolo [1,2-c:2',1'-f][1,3,2]diazaborinin-10-yl)aniline:** To a solution of 4-(5,5-difluoro-1,3,7,9-tetramethyl-5H-4λ<sup>4</sup>,5λ<sup>4</sup>-dipyrrolo[1,2-c:2',1'-f][1,3,2]diazaborinin-10-yl)-*N*-(2-nitrobenzyl)aniline (50mg, 0.11 mmol) in EtOH (8mL) were added NH<sub>2</sub>NH<sub>2</sub>.H<sub>2</sub>O (95μL) and Pd/C (10.11mg, 0.01 mmol). The reaction mixture was heated at reflux under Ar atmosphere for two hours, then it was cooled to room temperature and filtered. The solids were washed with DCM. The resultant residue was purified by column chromatography. (2:1 (Hexane:Ethyl acetate) to afford **BOD-SYR** as orange solid (20 mg, 40 % yield). <sup>1</sup>H NMR (400MHz, CDCl<sub>3</sub>) δ = 7.23 - 7.15 (m, 2 H), 7.07 (td, *J* = 2.3, 8.6 Hz, 2 H), 6.81 - 6.74 (m, 4 H), 5.98 (s, 2 H), 4.26 (br. s., 2 H), 4.07 (br. s, 2 H), 3.96 (br. s, 1 H), 2.55 (s, 6 H), 1.51 (s, 6 H). <sup>13</sup>C NMR (100MHz, CDCl<sub>3</sub>) δ = 154.9, 148.8, 145.6, 143.2, 142.6, 130.1, 129.2, 129.0, 124.3, 122.4, 120.9, 118.6, 116.1, 113.8, 46.8, 14.8, 14.6. HRMS (QTOF): *m/z* Calcd. For C<sub>26</sub>H<sub>27</sub>BF<sub>2</sub>N<sub>4</sub>: 444.2297 [M-H]<sup>+</sup>, Found: 445.2443 [M-H]<sup>+</sup>.

### 2.3.5. Synthesis of BOD-UREA

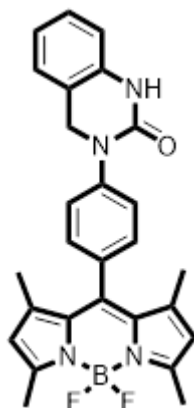


Figure 2.6. 3-(4-(5,5-difluoro-1,3,7,9-tetramethyl-5H-4 $\lambda$ <sup>4</sup>,5 $\lambda$ <sup>4</sup>-dipyrrolo[1,2-c:2',1'-f][1,3,2]diazaborinin-10-yl)phenyl)-3,4-dihydroquinazolin-2(1H)-one

**3-(4-(5,5-difluoro-1,3,7,9-tetramethyl-5H-4 $\lambda$ <sup>4</sup>,5 $\lambda$ <sup>4</sup>-dipyrrolo[1,2-c:2',1'-f][1,3,2]diazaborinin-10-yl)phenyl)-3,4-dihydroquinazolin-2(1H)-one:** <sup>1</sup>H NMR (400MHz, CDCl<sub>3</sub>)  $\delta$ = 7.54 (d,  $J$ = 8.4, 2H), 7.32 (d,  $J$ = 8.4, 2H), 7.17-7.15 (m, 1H), 7.05-7.02 (m, 1H), 6.88 (s, 1H), 6.79-6.77 (m, 1H), 5.99 (s, 2H), 4.91 (s, 2H), 2.56 (s, 6H), 1.47 (s, 6H).

### 2.4. Determination of Quantum Yield

Fluorescence quantum yields of **BOD-SYR** was determined by using optically matching solutions of Rhodamine 6G ( $\Phi_F$ =0.95 in ethanol) as a standard. The quantum yield was calculated according to the equation;  $\Phi_F(X) = \Phi_F(S) (A_S F_X / A_X F_S) (n_X / n_S)^2$ . Where  $\Phi_F$  is the fluorescence quantum yield, A is the absorbance at the excitation wavelength, F is the area under the corrected emission curve, and n is the refractive index of the solvents used. Subscripts S and X refer to the standard and to the unknown, respectively.

## 2.5. Determination of Detection Limit

The detection limit was calculated based on the fluorescence titration. To determine the detection limit, the emission intensity of **BOD-SYR** (10.0  $\mu\text{M}$ ) without phosgene was measured by 10 times and the standard deviation of blank measurements was determined. Under the present conditions, a good linear relationship between the fluorescence intensity and phosgene concentration could be obtained in the 0,5-1  $\mu\text{M}$  ( $R = 0.9814$ ). The detection limit is then calculated with the equation: detection limit =  $3\sigma_{bi}/m$ , where  $\sigma_{bi}$  is the standard deviation of blank measurements;  $m$  is the slope between intensity versus sample concentration.

## CHAPTER 3

### RESULT AND DISCUSSION

In this study, it is presented that the design, synthesis, and spectral investigation of a new probe which undergoes a unique reaction process to determine phosgene with excellent selectivity over other acetyl chloride species. For this probe design, I used a boron–dipyrromethene (BODIPY) dye to utilize its outstanding photophysical properties, and it is desired that its *o*-aminobenzyl amine group can be used as the phosgene-specific reactive unit, which means that this is the first time it is used to determine phosgene sensing (Sayar et al. 2018).

Expecting that when the phosgene reacts with the probe's reactive site to carry out a cyclisation reaction, the PET process is blocked (Fig 3.1), which causes a turn-on fluorescent response.

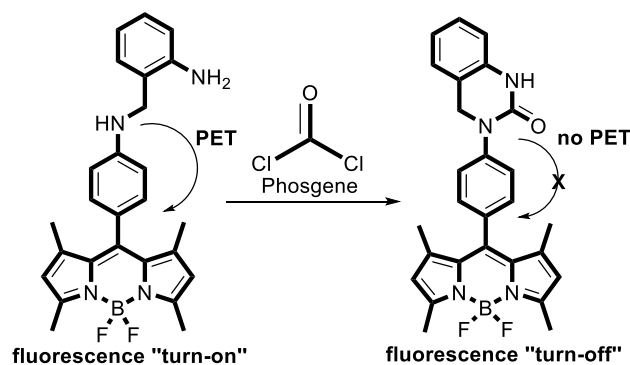


Figure 3.1. Reaction-Based Detection of Phosgene

For the spectral investigation, triphosgene was used as a source of phosgene which provides safe handling of phosgene and in the presence of tertiary amines, triphosgene turns into phosgene easily. Also, after synthesis of the probe, to choose the best solvent, different organic solvents like  $\text{CHCl}_3$ , DMF, THF and ACN were evaluated and it was determined that ACN was more convenient than others in terms of the spectroscopic response of each measurement.

To examine the spectroscopic response of **BOD-SYR** with the addition of phosgene and other species by using same reactive environment, ultraviolet-visible and fluorescence spectroscopy were used.

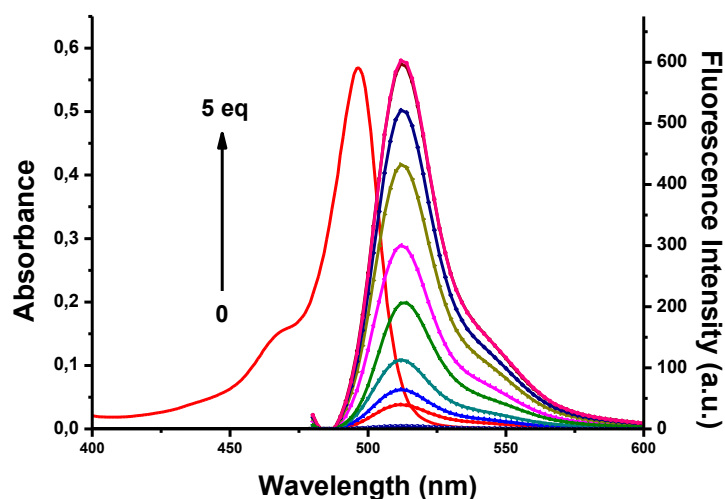


Figure 3.2. Absorbance and Fluorescence Spectra of **BOD-SYR** upon Gradual Addition of a Solution of Triphosgene (0–5 equiv) in Acetonitrile ( $\text{CH}_3\text{CN}$ ), ( $\lambda_{\text{exc}}=460$  nm). Inset: Fluorescence Response of **BOD-SYR** Towards Phosgene.



Figure 3.3. Naked eye Appearance in the Absence and the Presence of Phosgene

According to the result of UV and fluorescence measurements, the **BOD-SYR** solution (i.e., acetonitrile, with 0.1%  $\text{Et}_3\text{N}$ ) shows no emission ( $\Phi_{\text{F}}=0.005$ ) in the visible region because of the PET-process from the meso-amine unit which quenches spectroscopic response. However, with the addition of triphosgene (1 equiv.), PET-process is blocked, and an intense emission band is seen at 511 nm (Figure 3.2).

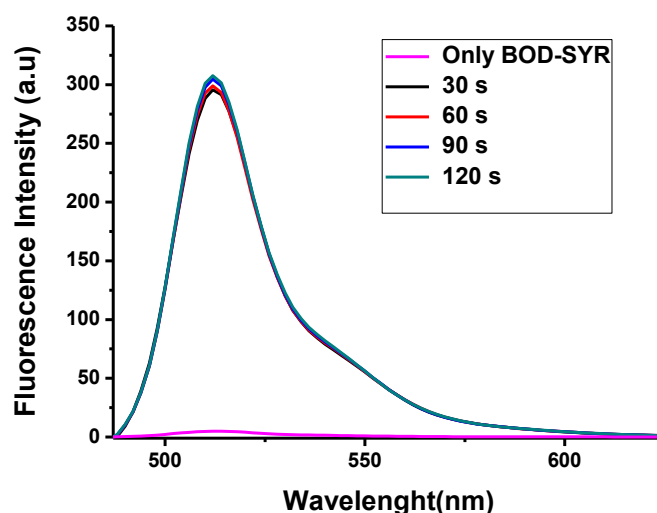


Figure 3.4. Time-Dependent Fluorescence Change **BOD-SYR** in  $\text{CH}_3\text{CN}$  (20 Mm) in the Presence of Triphosgene (5 equiv.) in  $\text{CH}_3\text{CN}$  containing TEA (0.1%).

It is obvious that the spectroscopic response of the probe is rapid that means the saturation of signal intensity accomplishes within seconds (Figure 3.4).

With the systematic addition of phosgene, the emission band at 511 nm increased linearly, and its intensity peaked with the addition of 5 equiv. of phosgene, with an enhancement factor of more than 300-fold (Figure 3.5).

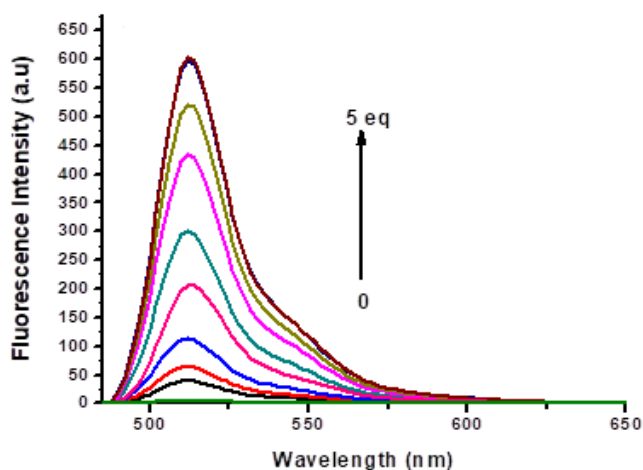


Figure 3.5. Fluorescence Spectra of **BOD-SYR** in  $\text{CH}_3\text{CN}$  (20 mM) upon Gradual Addition of a Solution of Triphosgene (0–5 equiv, From Bottom to Top) in  $\text{CH}_3\text{CN}$  Containing TEA (0.1%). ( $\lambda_{\text{exc}} = 460 \text{ nm}$ ).



After titration experiment, according to collected analytical data, limit of detection is calculated as 176 nM (Figure 3.6).

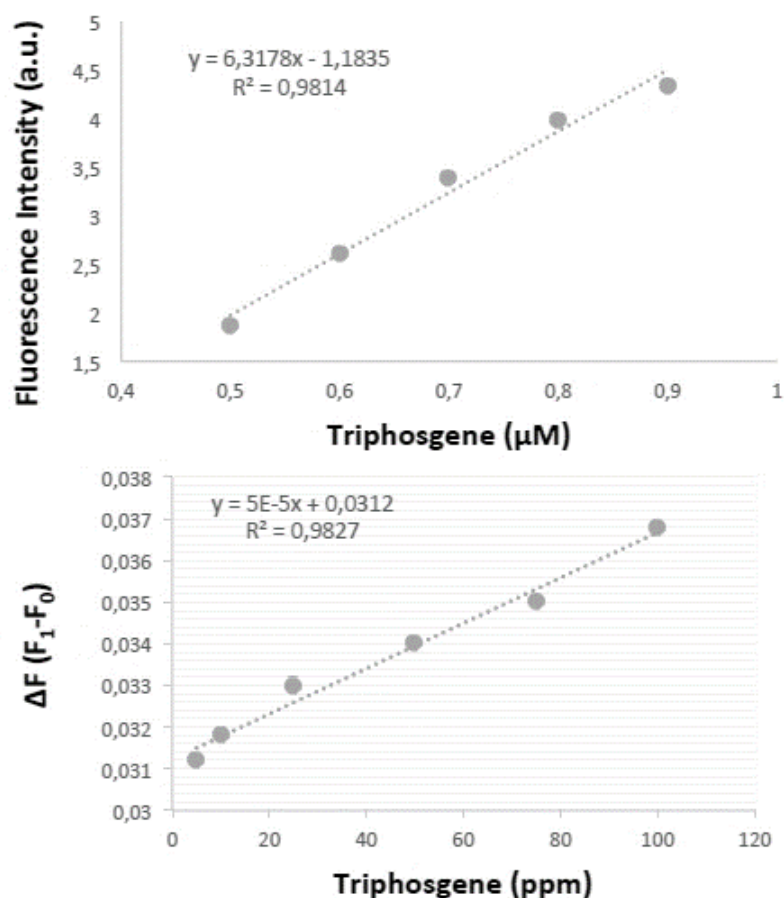


Figure 3.6. Graphs Used for Calculation of Detection Limit

By the systematic addition of the phosgene, solution's emission was getting become green, this means that there was a reaction. To be sure about that, this new compound was monitored on a TLC plate, it was also proof of the formation of a new BODIPY derivative. To confirm the this BODIPY derivative, after purification by column chromatography, nuclear magnetic resonance spectroscopy (NMR) and mass analysis were applied and the result of these analysis, the compound structure was confirmed as the cyclization product of the probe. **BOD-SYR**'s primary aryl amine undergoes nucleophilic substitution reaction with phosgene that it promoted an intramolecular cyclisation to yield a new BODIPY structure, **BOD-SYR** ( $\Phi F=0.52$ ), with a cyclic urea on the meso position. With acetyl chloride ( $\text{CH}_3\text{COCl}$ ), the monosubstitution of the primary amine eliminated a step of cyclisation, which clearly indicates the probe's exceptional selectivity toward phosgene (Figure 3.7).

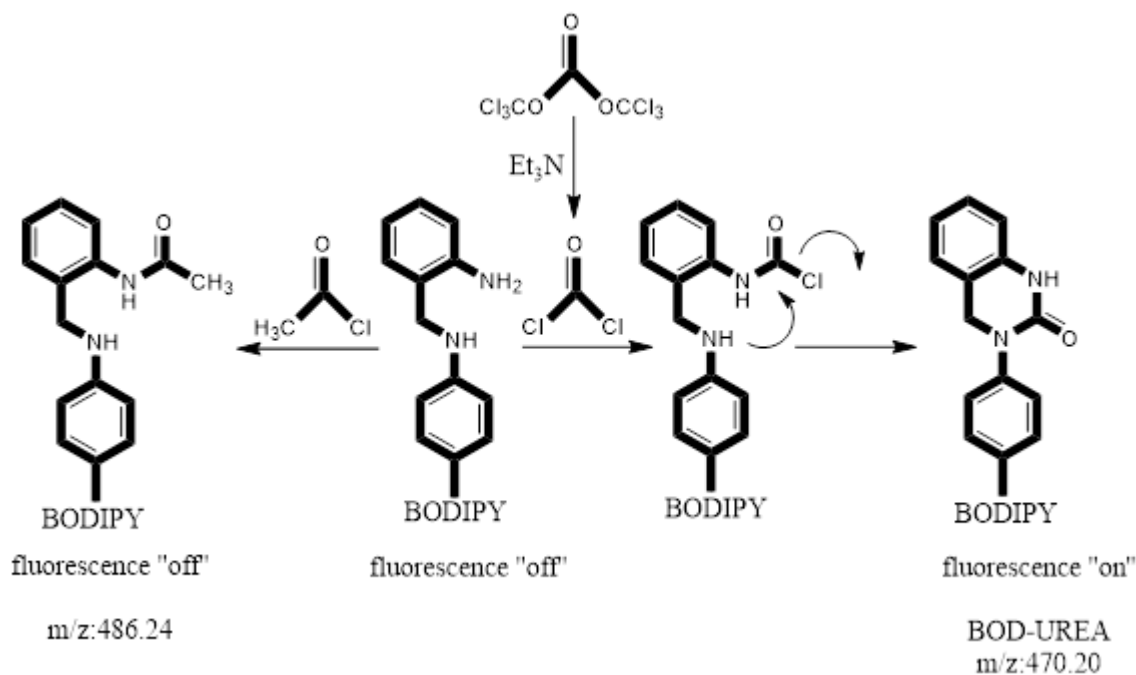


Figure 3.7. Proposed Reaction Mechanism for the Trapping of Triphosgene.

Moreover, the probe's spectroscopic behavior was investigated in the presence of other potentially reactive species. Any significant change was not observed in fluorescence by using same sensing environment for other reactive analytes, including acetyl chloride ( $\text{CH}_3\text{COCl}$ ), oxalyl chloride [ $(\text{COCl})_2$ ], thionyl chloride ( $\text{SOCl}_2$ ), phosphorus oxychloride ( $\text{POCl}_3$ ), tosyl chloride ( $\text{TsCl}$ ), and the nerve agent mimic like diethylchlorophosphate (DCP) (Figure 3.8).

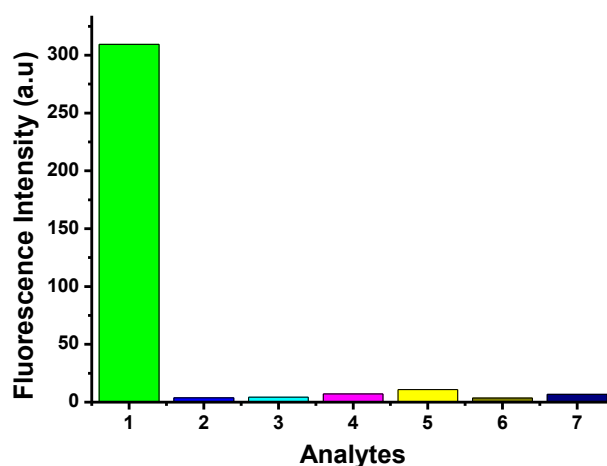


Figure 3.8. Fluorescence intensity change of BOD-SYR ( $20 \mu\text{M}$ , in  $\text{CH}_3\text{CN}/\text{TEA}$  (0.1%)) recorded 2 min. after the addition of various analytes (10 eq.) ( $\lambda_{\text{ex}} = 460 \text{ nm}$ ). (1) Phosgene, (2)  $\text{POCl}_3$ , (3) DCP, (4)  $(\text{COCl})_2$ , (5)  $\text{SOCl}_2$ , (6)  $\text{TsCl}$ , (7)  $\text{CH}_3\text{COCl}$ .

## CHAPTER 4

### CONCLUSION

To conclude, the phosgene-specific fluorescent probe was designed and synthesized and its sensing competences towards other potential reactive species. BODIPY dye was used as a visible light harvesting chromophore and new generation reactive motif, o-aminobenzyl amine unit which was used for the first time for phosgene sensor development.

Before the addition of phosgene, **BOD-SYR** has exhibited no emission because of PET process. Although potential reactive species were added, there was no spectral response especially toward nerve agent mimic, DCP which was the main concern about this probe development.

Our novel probe is based on six membered cyclization reaction and at the end of this reaction, **BOD-UREA** was produced which was confirmed by using HRMS and NMR analysis. Also, this cyclization reaction process exhibits comparable analytical performance with the previously described systems and probe shows a remarkable change in fluorescence emission toward phosgene rather than other potential reactive species and the nerve agents mimic, DCP with high sensitivity and selectivity even with an advanced response time (< 10 s) and detection limit as 176 nM.

## REFERENCES

- Alford, Raphael, Haley M. Simpson, Josh Duberman, G. Craig Hill, Mikako Ogawa, Celeste Regino, Hisataka Kobayashi, and Peter L. Choyke. 2009. "Toxicity of Organic Fluorophores Used in Molecular Imaging: Literature Review." *Molecular Imaging* 8 (6): 7290.2009.00031. <https://doi.org/10.2310/7290.2009.00031>.
- Bast, Cheryl B., and Dana F. Glass. 2009. "Phosgene." In *Handbook of Toxicology of Chemical Warfare Agents*, 321–30. Elsevier. <https://doi.org/10.1016/B978-0-12-374484-5.00023-7>.
- Chen, Liyan, Di Wu, Jong Man Kim, and Juyoung Yoon. 2017. "An ESIPT-Based Fluorescence Probe for Colorimetric, Ratiometric, and Selective Detection of Phosgene in Solutions and the Gas Phase." *Analytical Chemistry* 89 (22): 12596–601. <https://doi.org/10.1021/acs.analchem.7b03988>.
- Cucinell, Samuel A., and Edgewood Arsenal. 1974. "Review of the Toxicity of Long-Term Phosgene Exposure." *Archives of Environmental Health: An International Journal* 28 (5): 272–75. <https://doi.org/10.1080/00039896.1974.10666485>.
- Das, Sudipta, Mili Dutta, and Debasis Das. 2013. "Fluorescent Probes for Selective Determination of Trace Level Al<sup>3+</sup>: Recent Developments and Future Prospects." *Analytical Methods* 5 (22): 6262. <https://doi.org/10.1039/c3ay40982a>.
- Hu, Ying, Liyan Chen, Hyeseung Jung, Yiyang Zeng, Songyi Lee, Kunemadhalli Mathada Kotraiah Swamy, Xin Zhou, Myung Hwa Kim, and Juyoung Yoon. 2016. "Effective Strategy for Colorimetric and Fluorescence Sensing of Phosgene Based on Small Organic Dyes and Nanofiber Platforms." *ACS Applied Materials and Interfaces* 8 (34): 22246–52. <https://doi.org/10.1021/acsami.6b07138>.
- Loudet, Aurore, and Kevin Burgess. 2007. "BODIPY Dyes and Their Derivatives: Syntheses and Spectroscopic Properties." *Chemical Reviews* 107 (11): 4891–4932. <https://doi.org/10.1021/cr078381n>.
- Sayar, Melike, Erman Karakuş, Tuğrul Güner, Busra Yildiz, Umit Hakan Yildiz, and Mustafa Emrullahoğlu. 2018. "A BODIPY-Based Fluorescent Probe to Visually

- Detect Phosgene: Toward the Development of a Handheld Phosgene Detector.” *Chemistry - A European Journal* 24 (13): 3136–40. <https://doi.org/10.1002/chem.201705613>.
- Treibs, Alfred, and Franz-heinrich Kreuzer. 1969. “Elektrophile Substitution an Pyrrolen Mit Acylchloriden.” *Justus Liebigs Annalen Der Chemie* 721 (1): 105–15. <https://doi.org/10.1002/jlac.19697210115>.
- Ulrich, Gilles, Raymond Ziessel, and Anthony Harriman. 2008. “The Chemistry of Fluorescent Bodipy Dyes: Versatility Unsurpassed.” *Angewandte Chemie - International Edition* 47 (7): 1184–1201. <https://doi.org/10.1002/anie.200702070>.
- Wang, Shao-Lin, Lin Zhong, and Qin-Hua Song. 2017. “A Ratiometric Fluorescent Chemosensor for Selective and Visual Detection of Phosgene in Solutions and in the Gas Phase.” *Chemical Communications* 53 (9). Royal Society of Chemistry: 1530–33. <https://doi.org/10.1039/C6CC09361B>.
- Wood, EJ. 1994. “Molecular Probes: Handbook of Fluorescent Probes and Research Chemicals: By R P Haugland. Pp 390. Interchim (Molecular Probes Inc, PO Box 22010 Eugene, OR 97402-0414, USA, or 15 Rue Des Champs, 92600 Asnieres, Paris). 1992–1994. \$15.” *Biochemical Education* 22 (2). No longer published by Elsevier: 83. [https://doi.org/10.1016/0307-4412\(94\)90083-3](https://doi.org/10.1016/0307-4412(94)90083-3).
- Wood, Tabitha E., and Alison Thompson. 2007. “Advances in the Chemistry of Dipyrrins and Their Complexes.” *Chemical Reviews* 107 (5): 1831–61. <https://doi.org/10.1021/cr050052c>.
- Wu, Xuanjun, Zhisheng Wu, Yuhui Yang, and Shoufa Han. 2012. “A Highly Sensitive Fluorogenic Chemodosimeter for Rapid Visual Detection of Phosgene.” *Chemical Communications* 48 (13): 1895. <https://doi.org/10.1039/c2cc17411a>.
- Xia, Hong-Cheng, Xiang-Hong Xu, and Qin-Hua Song. 2017. “Fluorescent Chemosensor for Selective Detection of Phosgene in Solutions and in Gas Phase.” *ACS Sensors* 2 (1): 178–82. <https://doi.org/10.1021/acssensors.6b00723>.
- Zhang, Hexiang, and Dmitry M Rudkevich. 2007. “A FRET Approach to Phosgene Detection.” *Chemical Communications (Cambridge, England)*, no. 12: 1238–39.

<https://doi.org/10.1039/b614725a>.

Zhang, Yuanlin, Aidong Peng, Xiaoke Jie, Yanlin Lv, Xuefei Wang, and Zhiyuan Tian. 2017. “A BODIPY-Based Fluorescent Probe for Detection of Subnanomolar Phosgene with Rapid Response and High Selectivity.” *ACS Applied Materials & Interfaces* 9 (16): 13920–27. <https://doi.org/10.1021/acsami.7b02013>.

Zhou, Xin, Yiying Zeng, Chen Liyan, Xue Wu, and Juyoung Yoon. 2016. “A Fluorescent Sensor for Dual-Channel Discrimination between Phosgene and a Nerve-Gas Mimic.” *Angewandte Chemie International Edition* 55 (15): 4729–33. <https://doi.org/10.1002/anie.201601346>.

# APPENDIX A

## $^1\text{H-NMR}$ AND $^{13}\text{C-NMR}$ SPECTRA OF COMPOUNDS

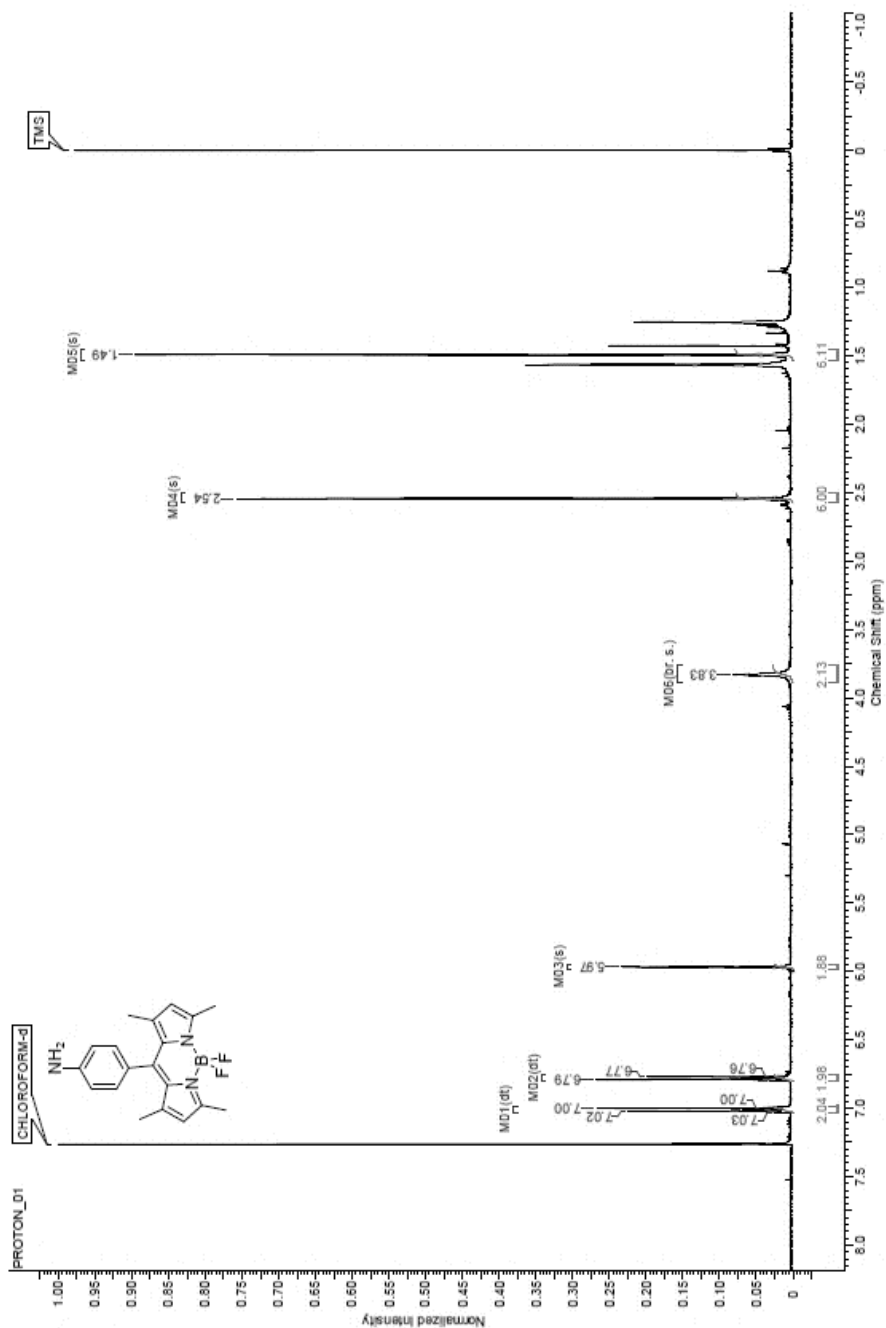


Figure A 1.  $^1\text{H-NMR}$  of BOD-NH<sub>2</sub>.

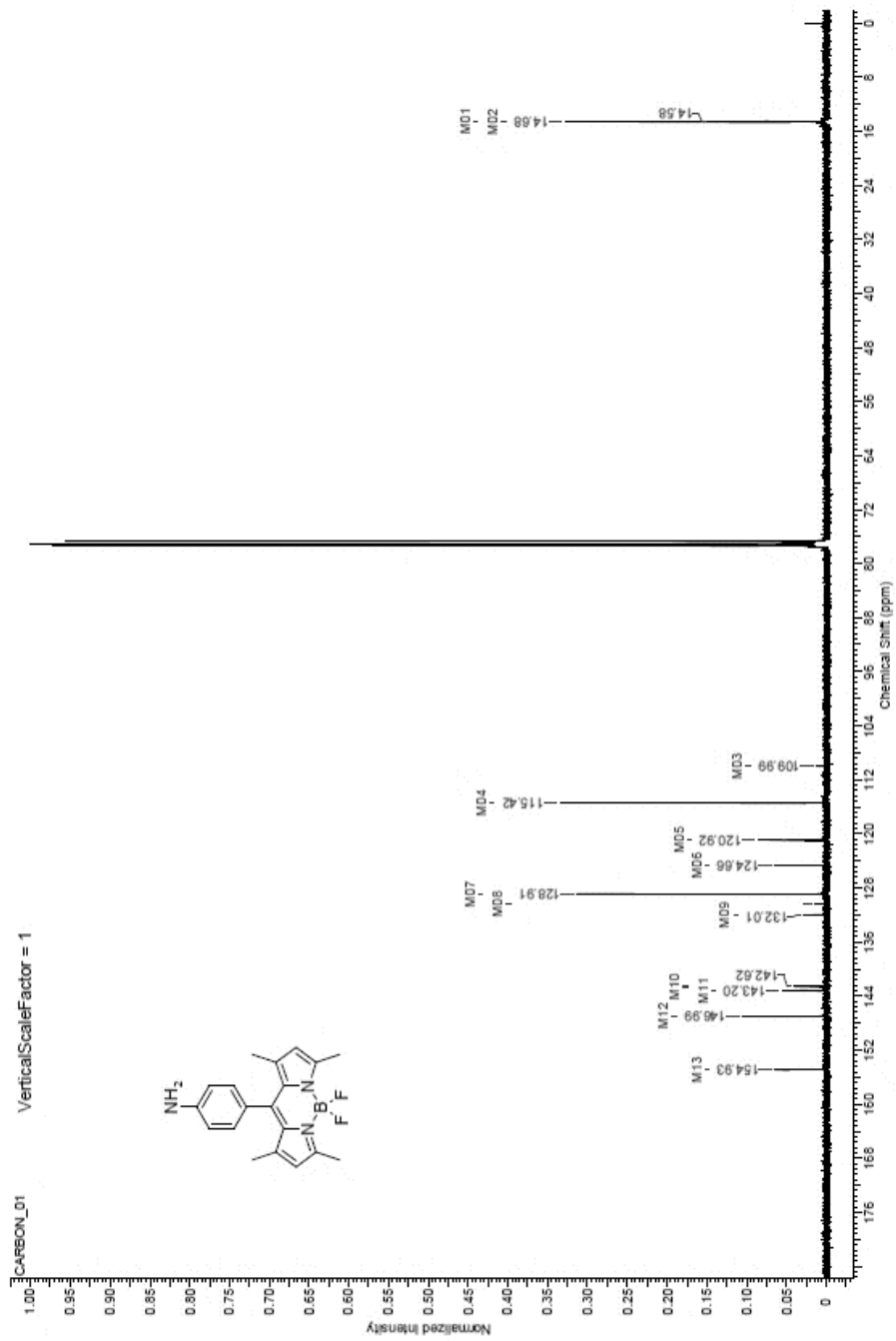


Figure A 2.  $^{13}\text{C}$  NMR of BOD-NH<sub>2</sub>.



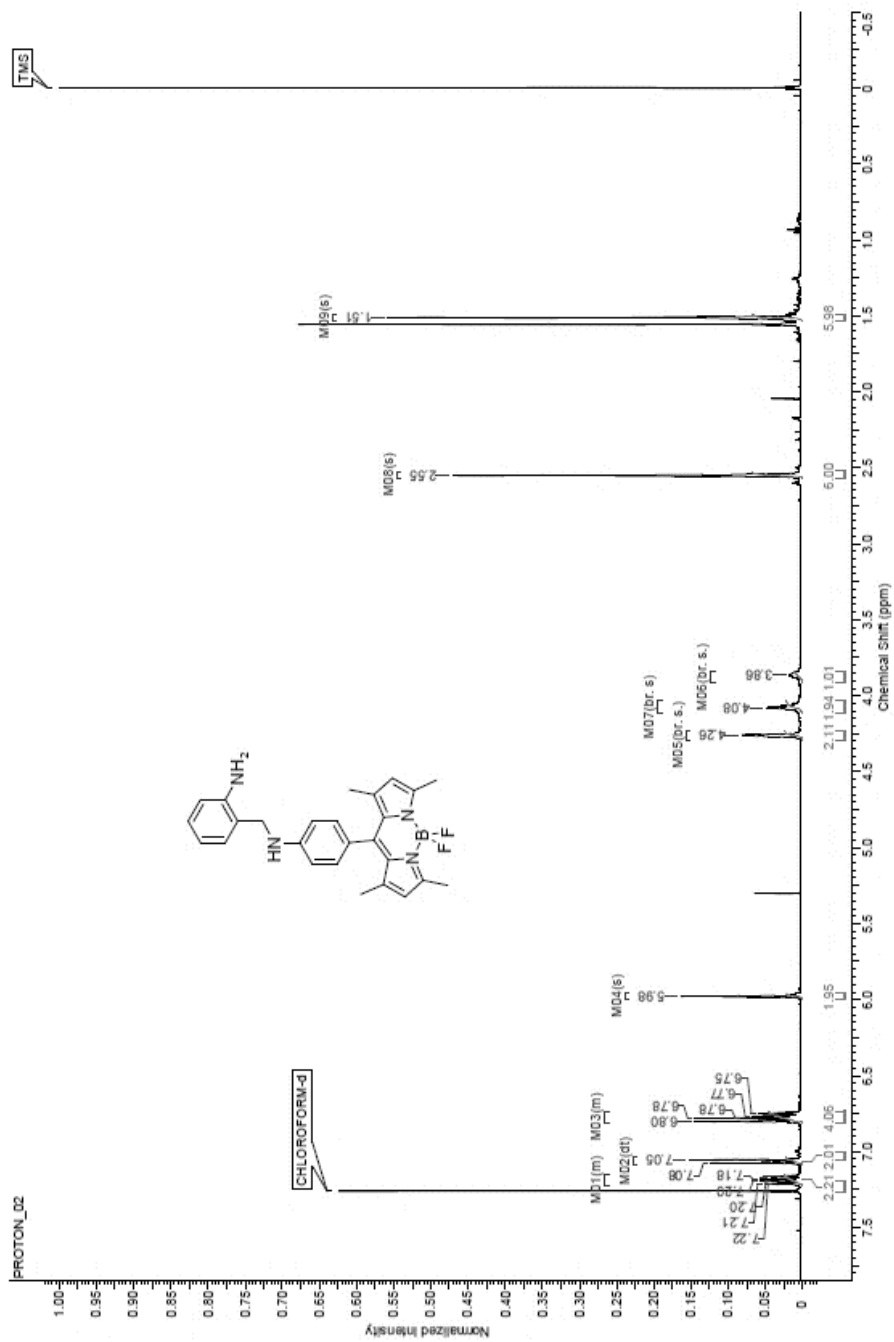


Figure A 3. <sup>1</sup>H NMR of BOD-SYR.

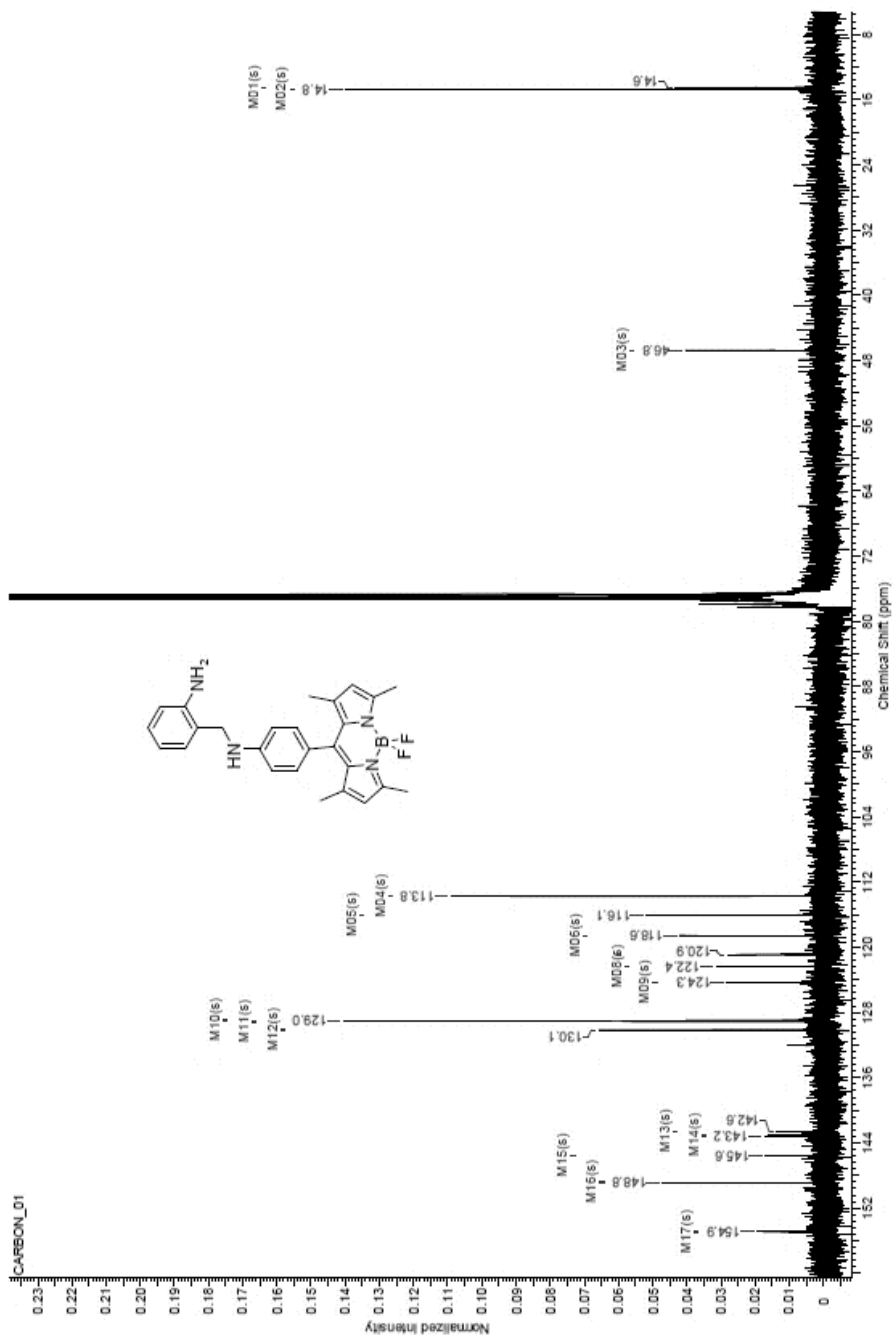


Figure A 4. <sup>13</sup>C NMR of BOD-SYR.

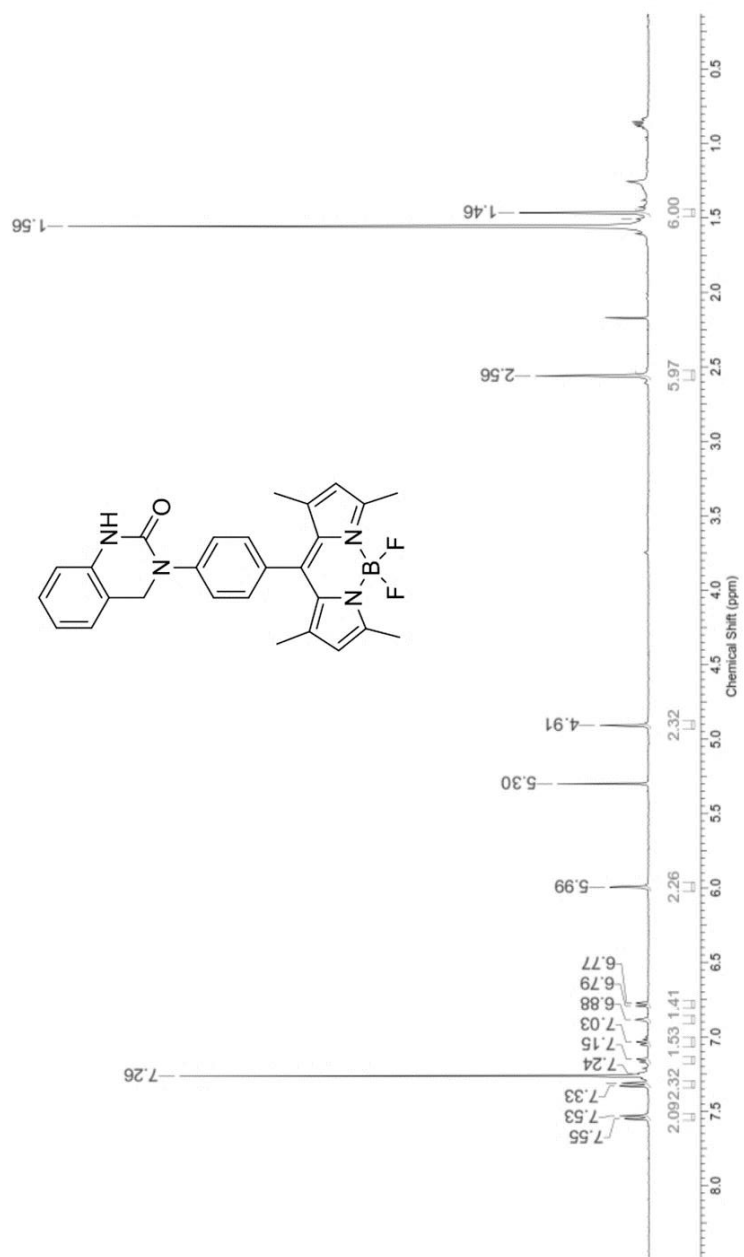


Figure A 5.  $^1\text{H}$  NMR of BOD-UREA.

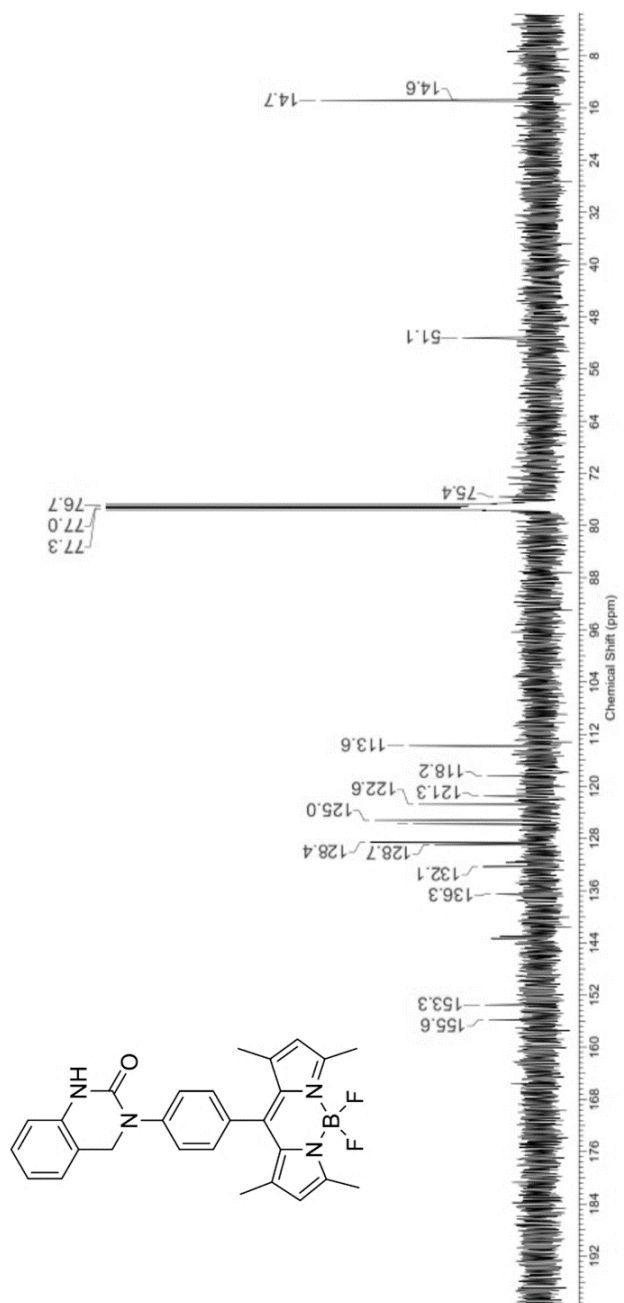


Figure A 6. <sup>13</sup>C NMR of BOD-UREA.

## APPENDIX B MASS SPECTRA OF COMPOUNDS

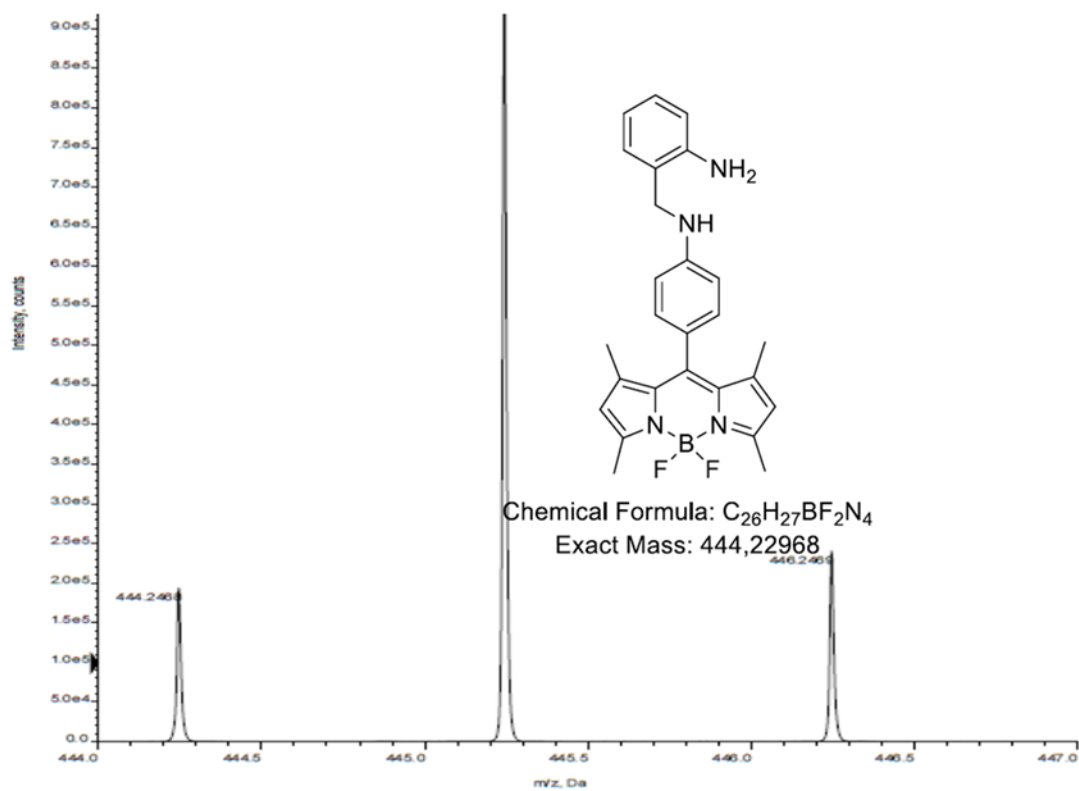


Figure B 1. HRMS of BOD-SYR.

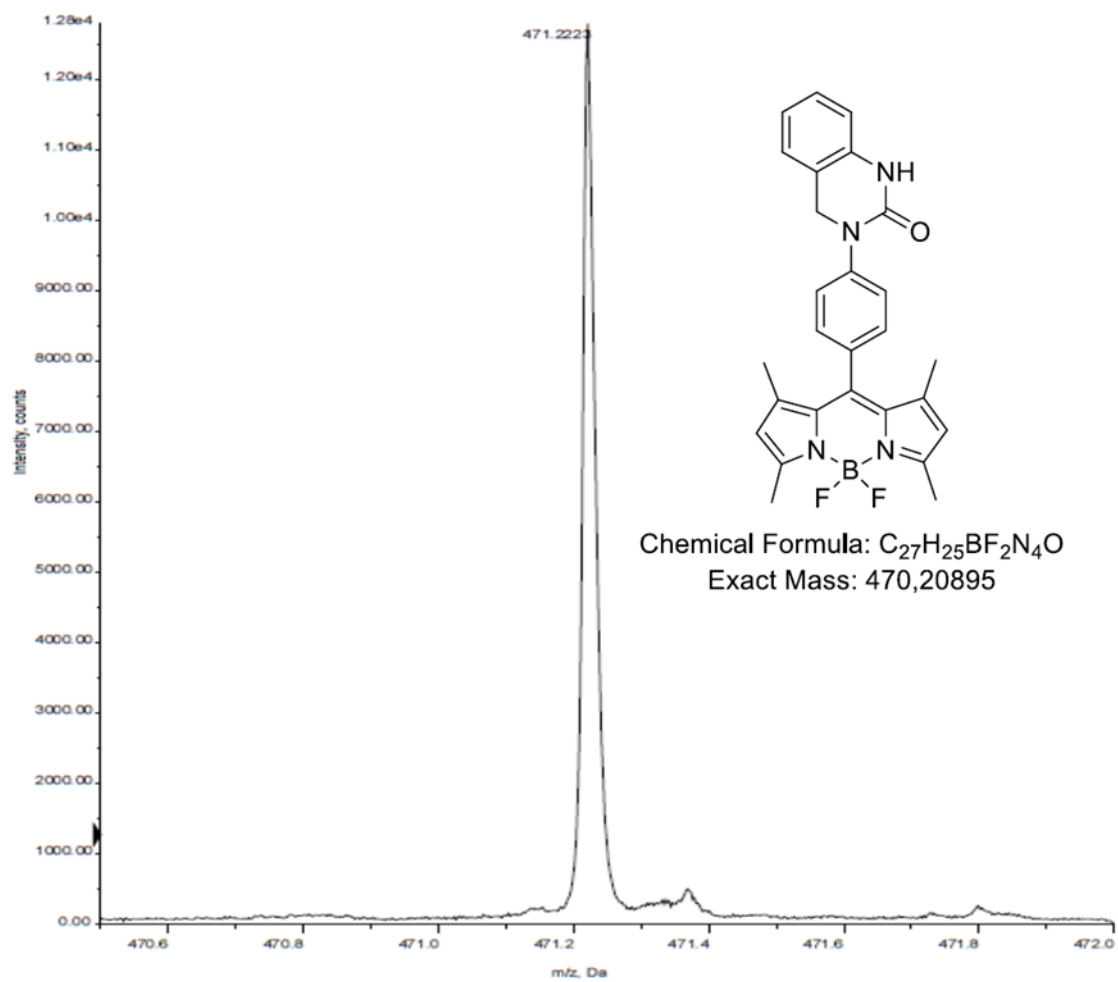


Figure B 2. HRMS of BOD-UREA.